

A Climate Transect through Tropical Montane Rain Forest in Hawaii

JAMES O. JUVIK AND DENNIS NULLET

Department of Geography, University of Hawaii at Hilo, Hilo, Hawaii

(Manuscript received 19 October 1993, in final form 14 February 1994)

ABSTRACT

Two years of climate data from a transect of three surface meteorological stations on the windward slopes of Mauna Loa, Hawaii, are analyzed. The stations constitute a transect between 700 and 1640 m through the wet, montane rain forest zone below the trade-wind inversion. Data are compared with previous short-term measurements for the area, and previously unreported climate elements such as photosynthetically active radiation and soil temperature are presented. While absolute values vary between the sites, annual and diurnal climate patterns for the sites are remarkably similar, despite the altitudinal range involved and the close proximity of the trade-wind inversion level to the upper station.

1. Introduction

In this report, we analyze two years of climate measurements at three sites between 700 and 1640 m on the windward slope of Mauna Loa volcano, on the island of Hawaii. This climate monitoring transect was established as part of a larger interdisciplinary study of environmental factors [e.g., climate, relief, parent material, organisms, and time; "state factors", sensu Jenny (1980)] that control tropical ecosystem structure and function. The windward slope of Mauna Loa volcano is covered by a well-replicated age series of recent volcanic substrates (historically dated lava flows) in close spatial proximity. In addition, these volcanic deposits typically transect the mountain slope along very steep topo-climate gradients. For example, annual rainfall on the windward slope of Mauna Loa ranges from more than 7000 mm yr⁻¹ near 1000 m to less than 500 mm yr⁻¹ near the mountain summit at 4170 m (Fig. 1). Ecosystem development on the windward slope of Mauna Loa thus exists as a mosaic of native plant communities responding to a complex climate-substrate age matrix (see Vitousek et al. 1992; Mueller-Dombois 1992). The site provides a unique opportunity to isolate the factors contributing to the rate and character of primary ecological succession by permitting both age constant (upslope-downslope vegetation differences on the same lava flow under different climate conditions) and climate constant (across slope at the same elevation on different age lava flows) comparisons of ecosystem development.

The major goal of this article is to describe quantitatively the general climate on the windward slopes of

Mauna Loa below an upper-level temperature inversion (the trade-wind inversion) using long-term measurements. A detailed climatic characterization of this poorly known mountain region can provide a better understanding of both the environmental controls on tropical montane ecosystem development and the hydrology of an important mountain watershed (particularly, the evaporation component of the montane forest water balance).

2. Physical setting

The island of Hawaii, southernmost in the Hawaiian archipelago and centered at 19°30'N, 155°30'W, lies in the trade-wind belt of the tropical North Pacific Ocean. The northeast trade winds prevail 80%–95% of the time in summer (May–September) but diminish in frequency during winter to as little as 50% in January (Blumenstock and Price 1967). The interaction of the island's five volcanic peaks (with two summits above 4100 m), the steady trade winds (typical azimuth 70°), and a persistent, upper-level subsidence temperature inversion (descending arm of the Hadley cell) present 70% of the time at mountain elevations between 1800 and 2400 m, creates a complex climatic pattern characterized by sharp climate gradients (Juvik et al. 1978). Rainfall is the most variable climate element over the island and has been the most intensively studied and monitored. Rainfall varies from over 7000 mm yr⁻¹ on the eastern slopes of the island to less than 250 mm yr⁻¹ in the dry, west coast rain shadow (see Fig. 1). On the windward slopes, orographic lifting of the onshore trades, aided by a daytime upslope sea breeze, produces rainfall maxima near the 1000-m elevation. The upper-level inversion inhibits vertical airflow on the upper slopes of Hawaii's large mountains and forces the trade winds around—rather than over—the island (Leopold

Corresponding author address: Dr. James O. Juvik, Dept. of Geography, University of Hawaii at Hilo, Hilo, HI 96720.

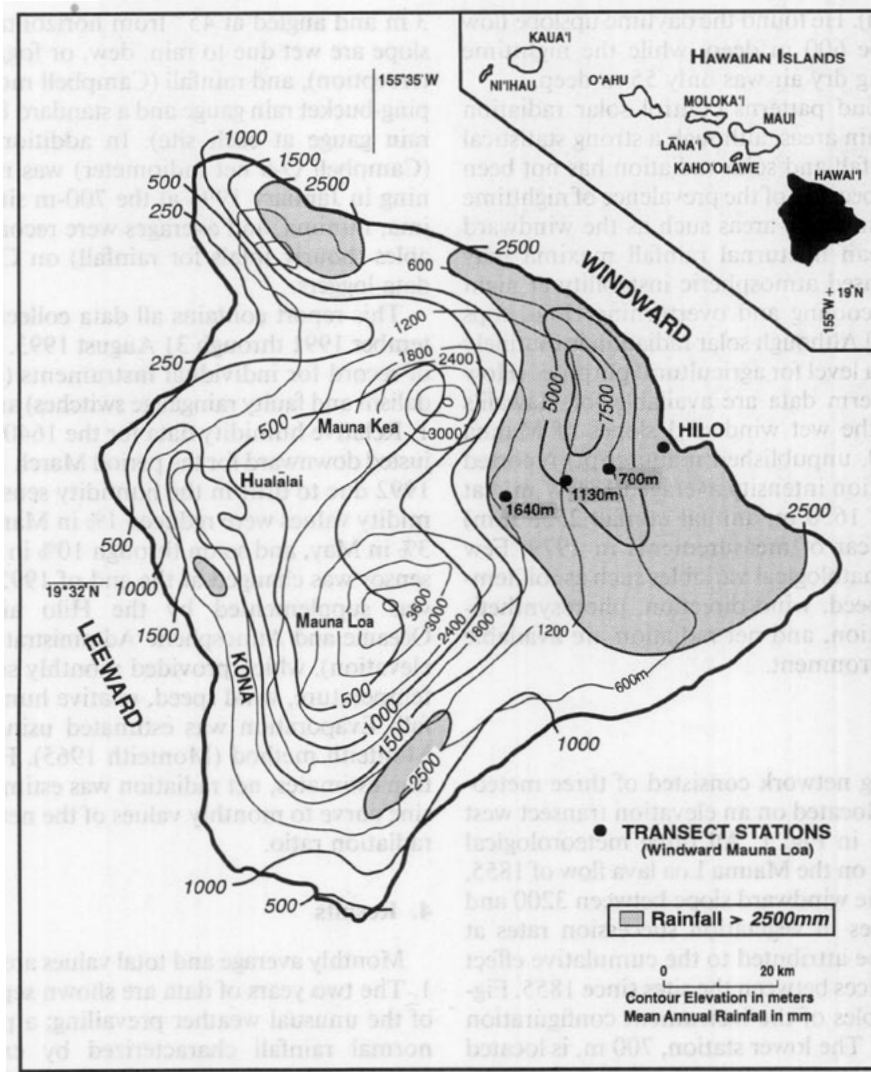


FIG. 1. Station locations, Hawaii. Mean annual rainfall (areas greater than 2500 mm yr⁻¹ shaded) from Giambelluca et al. (1986) and Armstrong (1983) (gauge network: $n = 392$; period base 1916–83).

1949). This flow pattern produces rainfall maxima below the inversion level on the windward slopes and very dry conditions above it (Fig. 1). Two previous, short-term collaborative projects have studied the character of orographic rainfall on the windward slope of Mauna Loa: Project Shower from October to December 1954 (Mordy 1957) and the Warm Rain Project during 11 July–24 August 1965 (Lavoie 1967a), which concentrated largely on cloud dynamics and physics.

The climatology of surface winds over the island is dominated by the interaction of the prevailing trade-wind flow and a diurnal land–sea breeze. Although the diurnal circulation is most strongly developed on the leeward slopes of the island, it is also evident on the windward side. Lavoie (1967b) reported a diurnal land–sea-breeze circulation above Hilo, a site exposed to prevailing onshore trade winds. The circulation cell was evident to almost 3-km height, although at higher

altitudes (above 380 m) it was represented only by a slackening or strengthening of the prevailing trades. The nighttime offshore surface wind had sufficient strength and duration to produce a resultant wind direction of 243° during 11 July–24 August 1965, in opposition to the synoptic resultant wind (above 500 m) of 77°–90°. A similar diurnal reversal of wind direction for sites inland and upslope of Hilo was found by Eber (1957) and Garrett (1980) even under strong (7–10 m s⁻¹) trade-wind conditions, based on short-term measurements. Garrett also related the growth, upslope penetration, and dissipation of orographic clouds on windward Mauna Loa to solar radiation and other meteorological variables based on measurements during 11 summer days. Above the upper-level temperature inversion on Mauna Loa, Mendonca (1969) used a captive balloon system to measure the depth of the diurnal circulation at Mauna Loa Observatory

(3400-m elevation). He found the daytime upslope flow of moist air to be 600 m deep, while the nighttime downslope flowing dry air was only 55 m deep.

Orographic cloud patterns control solar radiation receipt in mountain areas, although a strong statistical link between rainfall and solar radiation has not been found in Hawaii, because of the prevalence of nighttime rainfall maxima in some areas such as the windward coasts [Open ocean nocturnal rainfall maxima may result from increased atmospheric instability at night due to radiative cooling and overturning cloud tops (Schroeder 1994).] Although solar radiation is routinely measured near sea level for agricultural purposes (How 1978), few long-term data are available for Hawaii's mountains. For the wet windward slopes of Mauna Loa, Ekern (1980, unpublished manuscript) reported global solar radiation intensity averaged 171 W m^{-2} at Kulāni (elevation 1650 m; annual rainfall 2558 mm) based on a full year of measurements in 1979. Few data for other climatological variables such as soil temperature, wind speed, wind direction, photosynthetically active radiation, and net radiation are available for the study environment.

3. Data

The monitoring network consisted of three meteorological stations located on an elevation transect west of Hilo as shown in Fig. 1. All three meteorological stations were sited on the Mauna Loa lava flow of 1855, which descends the windward slope between 3200 and 500 m. Differences in vegetation succession rates at each station can be attributed to the cumulative effect of climate differences between the sites since 1855. Figure 2 gives examples of the instrument configuration and site exposure. The lower station, 700 m, is located in open scrub forest (*Metrosideros polymorpha* dominant) just below the elevation of maximum rainfall on the island (Fig. 2, bottom). The site has clear upslope and downslope exposure, with the tree canopy height just below that of the wind sensors at 3 m. The middle station, 1130 m, is located in scrub forest (*Metrosideros*) just above the elevation of windward slope rainfall maximum. This site also has clear exposures, although the wind sensor is near the level of the tree canopy and below some nearby emergents. The upper site at 1640 m is located in more open lava fields with mixed low shrubs and trees (Fig. 2, top).

Each station recorded global solar radiation (henceforth called "solar radiation," Campbell Scientific LI200S pyranometers), photosynthetically active radiation (PAR, Campbell LI190SB quantum sensors), air temperature and relative humidity at 2 m (initially Hygrometrix sensors, replaced with Vaisala HMP35C temperature and humidity probes in January 1993), wind direction and speed at 3 m (R. M. Young wind monitors), soil temperature at 1 cm (Campbell model 107 temperature probes), leaf wetness (percent of time Campbell model 237 leaf wetness sensors mounted at

3 m and angled at 45° from horizontal, facing downslope are wet due to rain, dew, or fog/cloud water interception), and rainfall (Campbell model TE-525 tipping-bucket rain gauge and a standard 8" manually read rain gauge at each site). In addition, net radiation (Campbell Q-6 net radiometer) was measured beginning in January 1993 at the 700-m site. Hourly maxima, minima, and averages were recorded for all variables (hourly totals for rainfall) on Campbell CR-10 data loggers.

This report contains all data collected from 1 September 1991 through 31 August 1993. Missing periods of record for individual instruments (due to site vandalism and faulty rain gauge switches) are given in Table 1. Relative humidity data for the 1640-m site were adjusted downward for the period March 1992–December 1992 due to drift in the humidity sensor. Average humidity values were reduced 1% in March, 2% in April, 3% in May, and so on through 10% in December. The sensor was changed at the end of 1992. Transect data was supplemented by the Hilo airport National Oceanic and Atmospheric Administration station (8-m elevation), which provided monthly summaries of air temperature, wind speed, relative humidity, and rainfall. Evaporation was estimated using the Penman–Monteith method (Monteith 1965). For the evaporation estimates, net radiation was estimated by fitting a sine curve to monthly values of the net radiation/solar radiation ratio.

4. Results

Monthly average and total values are shown in Table 1. The two years of data are shown separately because of the unusual weather prevailing; a period of below-normal rainfall characterized by extreme drought punctuated with heavy rains. Both years of measurement included El Niño–Southern Oscillation events that have been linked to dry weather in Hawaii (Chu 1989). Individual climate elements are discussed herein.

a. Radiation

As shown in Table 1, solar radiation receipt closely follows the predictable annual pattern, with winter values being about two-thirds of summer values. Average solar radiation increased with elevation, from 139 W m^{-2} at 700 m to 191 W m^{-2} at 1640 m, in tandem with decreasing rainfall and the increasing influence of the inversion in cloud suppression. The 191 W m^{-2} average at the upper station is somewhat higher than the 171 W m^{-2} average for 1979 at the same elevation at Kulāni (13 km south of the 1640-m station) reported by Ekern (1980, unpublished manuscript). The diurnal solar radiation pattern appears symmetric around the noon hour at all sites. This sets the solar radiation regime apart from leeward sites exposed to a dominant land–sea-breeze circulation that experience peak solar

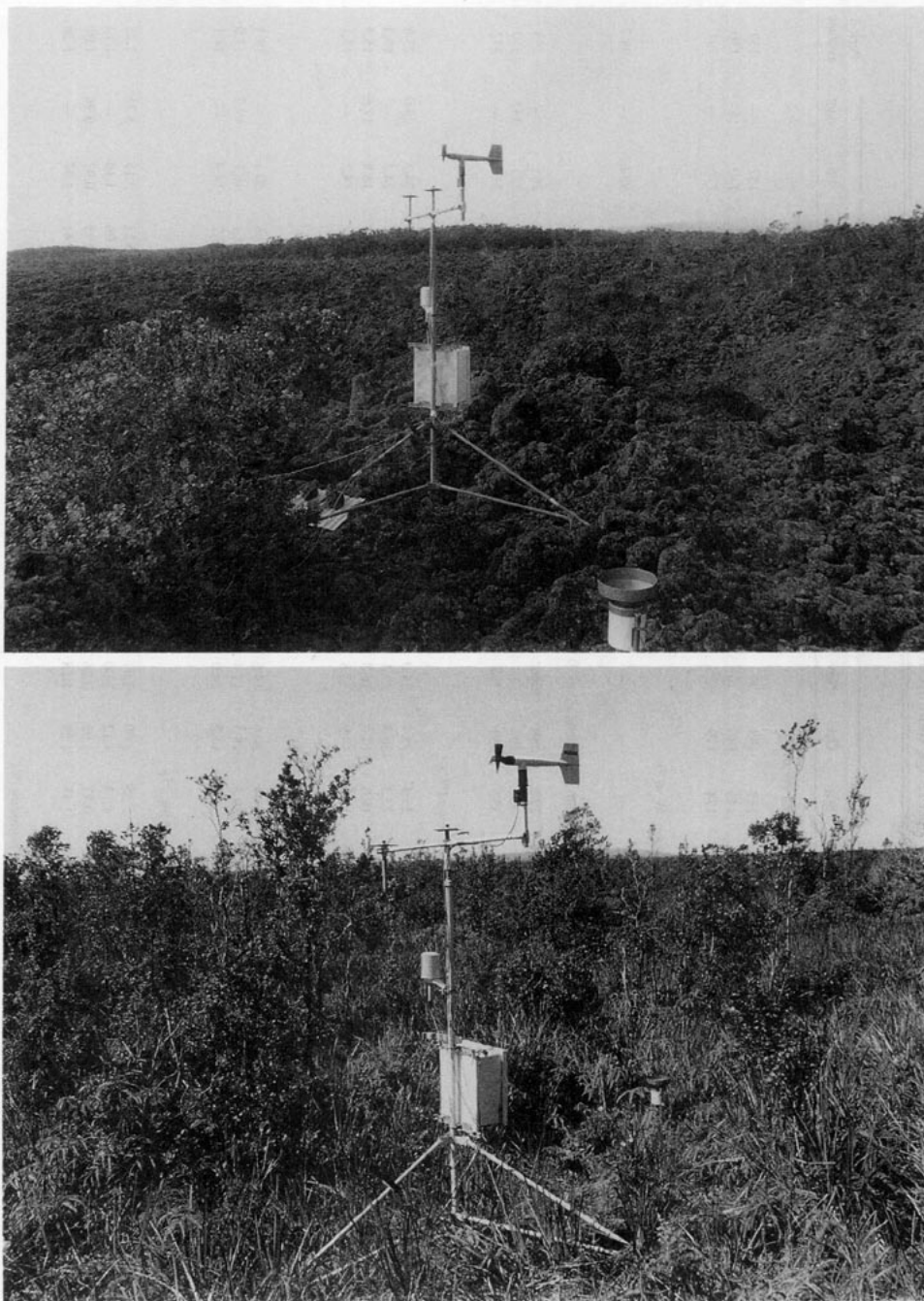


FIG. 2. Instrument configuration and exposure for climate stations at 1640 m (top) and 700 m (bottom) on 1855 Mauna Loa lava flow.

radiation before noon and then a drop off as late morning and afternoon cloud envelops the site (see Giambelluca and Nullet 1991; Juvik et al. 1993).

Photosynthetically active radiation ($0.4\text{--}0.7\ \mu\text{m}$) constitutes a fairly constant fraction of the total solar spectrum at each site for all months of the year. Assuming that $1\ \text{W m}^{-2}$ is approximately 4.6 micro-einsteins per second per square meter (Licor recommendation), the fraction PAR/solar radiation decreased

with elevation from 0.465 at 700 m to 0.423 at 1640 m, as shown in Fig. 3. The higher fraction at lower elevations could be attributed to a greater diffuse radiation component (richer in shorter wavelengths), increased infrared absorption in the marine air layer below the inversion, and greater ultraviolet scattering.

Net radiation was measured only at 700 m from January 1993 through July 1993. Values are given in Table 1. A distinct annual pattern in the ratio of net

TABLE 1. Data summary. Averages given for all climate elements except rainfall, for which total values are given. Only rainfall for months with complete records are shown. Averages for some months include incomplete data. Missing periods for partial months not shown in Table 1 are 700 m, 15 September–9 November 1991—all variables; 20 September–21 October 1992—air temperature (T_a), relative humidity (RH); 25–30 April 1993— T_a , RH, wind direction (WD); 18 May–5 July 1993— T_a , RH; 6–31 July 1993—RH; 1130 m, 18–30 May 1993— T_a , RH; 1640 m, 20 September–2 October 1992—all variables; 28 November–6 December 1992— T_a , RH; 11–15 May 1993—all variables; and 18–30 May 1993— T_a , RH. Average monthly rainfall for a two-year study period computed using a combination of manual and automatic rain gauge data are indicated by asterisks.

Elevation	1991												1992												Period average
	Sep	Oct	Nov	Dec	Jan	Feb	Mar	Apr	May	Jun	Jul	Aug	Sep	Oct	Nov	Dec	Jan	Feb	Mar	Apr	May	Jun	Jul	Aug	
	Global solar radiation ($W m^{-2}$)																								
700	183	—	116	114	132	142	162	135	157	155	153	130	137	138	97	97	115	130	163	166	155	155	132	—	139
1130	182	155	131	118	141	154	172	141	162	166	169	139	143	146	103	103	132	146	178	176	170	176	140	164	150
1640	232	186	174	146	181	197	223	188	192	208	208	182	174	179	125	126	175	201	233	228	222	230	176	—	191
700	—	—	—	—	—	—	—	—	—	—	—	—	—	—	—	—	63.4	79.2	107	116	112	115	98.6	—	98.7
	Net radiation ($W m^{-2}$)																								
700	419	—	263	259	293	315	362	306	356	355	345	287	292	288	206	201	229	260	326	321	300	311	265	—	298
1130	387	329	273	243	289	318	354	294	340	346	354	295	302	302	214	212	263	293	356	350	344	355	287	333	310
1640	471	381	356	291	366	397	440	367	380	400	402	348	337	354	238	237	240	391	444	432	410	433	310	—	372
	Photosynthetically active radiation ($\mu einsteins s^{-1} m^{-2}$)																								
10	24.9	24.6	24.3	22.7	21.8	21.9	22.4	22.4	23.8	24.6	24.6	25.1	25.4	25.4	24.0	23.1	21.7	21.2	22.0	23.1	22.9	24.1	24.3	25.0	23.6
700	19.6	—	18.7	17.0	16.3	16.3	16.4	17.1	18.9	19.0	19.5	19.9	22.3	20.3	21.1	21.2	17.8	16.2	18.9	19.5	24.1	—	24.2	—	19.3
1130	17.2	16.3	16.2	14.4	13.4	12.6	13.5	14.4	16.3	16.5	17.0	16.9	18.0	17.2	16.3	15.1	13.7	12.6	13.8	14.7	14.7	16.2	16.8	17.6	15.5
1640	15.0	14.1	14.0	11.9	10.9	11.8	11.0	12.1	14.1	14.0	14.8	14.7	16.4	14.9	13.8	12.4	11.4	10.7	11.7	12.2	12.0	13.9	14.2	—	13.1
	Air temperature ($^{\circ}C$)																								
700	21.4	—	19.1	17.8	16.4	16.5	17.4	17.8	19.4	20.3	20.9	20.8	21.4	20.6	19.6	18.6	16.9	16.6	18.5	19.5	19.5	20.6	20.5	—	19.1
1130	18.9	17.7	17.5	16.0	14.7	14.8	15.4	15.7	17.4	18.2	18.7	18.6	19.3	18.5	17.4	16.1	14.3	14.2	15.7	16.7	16.9	18.4	18.1	19.2	17.0
1640	16.1	15.2	15.0	12.6	11.0	13.0	13.4	12.7	14.4	15.2	15.6	15.5	17.0	15.2	14.0	13.0	10.9	12.4	13.4	14.1	13.3	15.2	14.9	—	14.1
	Soil temperature ($^{\circ}C$ at 1 cm)																								
10	3.22	3.13	3.00	3.49	3.58	3.84	3.62	3.31	3.49	3.31	3.27	3.04	3.35	3.00	2.91	2.86	3.26	3.40	3.40	3.35	3.31	3.17	3.13	3.35	3.28
700	1.40	—	1.16	1.10	1.32	1.17	1.22	1.15	1.10	1.04	1.02	0.96	1.13	1.12	1.00	1.09	1.29	1.18	1.18	1.22	1.14	1.06	1.10	—	1.14
1130	1.07	1.08	0.97	0.94	1.11	1.01	1.05	0.94	0.97	0.95	0.90	0.89	0.97	1.02	0.86	0.91	1.29	1.07	1.04	1.06	0.99	0.95	0.95	0.96	1.00
1640	1.49	1.24	1.24	1.24	1.32	1.46	1.45	1.39	1.55	1.44	1.47	1.37	1.47	1.29	1.18	1.15	1.33	1.39	1.52	1.59	1.31	1.41	1.47	—	1.38
	Wind speed ($m s^{-2}$)																								
10	81.8	79.4	82.6	79.6	72.9	71.6	70.3	76.5	76.3	79.6	82.6	83.4	82.5	77.5	84.3	83.6	75.1	71.5	77.1	77.1	78.1	80.4	83.0	—	78.6
700	88.3	—	90.4	92.3	88.8	89.8	90.9	94.2	93.4	95.5	95.4	96.3	95.3	93.4	94.5	93.8	85.2	87.2	88.2	87.9	91.3	—	—	—	91.6
1130	83.4	81.4	85.9	87.4	80.3	79.8	82.7	87.3	85.6	87.6	89.1	91.2	88.1	83.0	86.5	87.8	82.8	88.6	88.0	89.9	92.6	88.6	91.5	90.5	86.7
1640	88.6	88.6	90.8	95.1	84.0	79.3	88.7	92.9	90.8	93.3	92.0	92.5	90.7	87.9	89.6	79.9	74.6	76.3	79.9	86.4	93.7	90.0	94.7	—	97.8
	Relative humidity (%)																								

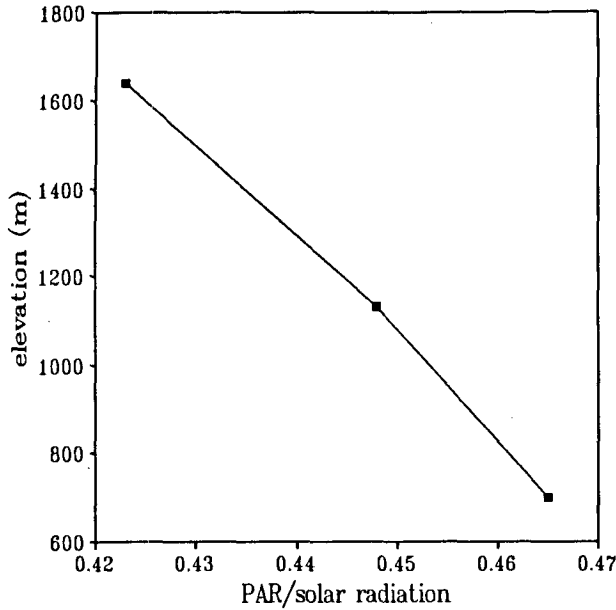


FIG. 3. Fraction PAR/solar radiation showing a decrease with elevation.

the tree canopy level at the two lower sites. No seasonal pattern in the monthly average wind speed appears evident along the transect.

The daily wind direction reversal prevailed for all 24 months of the study period for all sites as illustrated in Fig. 7, which shows the average wind direction at 0200 and 1400 LST for each month. This consistent diurnal pattern over the transect elevations based on long-term measurements supports the short-term observations of Garrett (1980) and Lavoie (1967b). Interestingly, the average 1400 LST azimuth converges

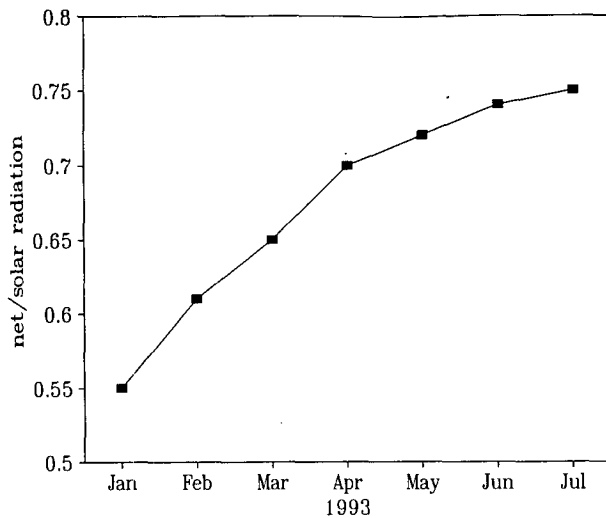


FIG. 4. Ratio of net to solar radiation showing seasonal pattern, with net radiation being a higher fraction of solar radiation in summer than winter.

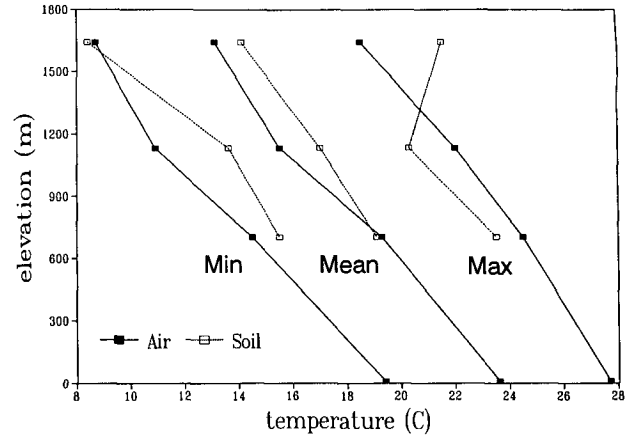


FIG. 5. Maximum, minimum, and average air and soil temperature lapse rates (average for the two-year sampling period). The range and lapse rates remain fairly constant with elevation except for soil temperature at the highest site.

for all sites to virtually due east as the upslope winds converge with the normal trade-wind flow. At night, however, the drainage wind direction stratifies by elevation and aspect, with the southerly component increasing with elevation. This matches the pattern expected of a pure, downslope drainage wind as the upper sites have a more northerly exposure.

d. Water

The rainfall profile during the study matched the pattern for long-term rainfall (see Fig. 1), with the maximum value occurring at 700 m. For the entire period, rainfall was below normal and included one of the driest winters (January–March 1992) on record at Hilo. Rainfall was about 80% of normal at Hilo, 62% at 700 m, 71% at 1130 m, and 52% at 1640 m. (See Table 1 for actual values.) A typical diurnal rainfall

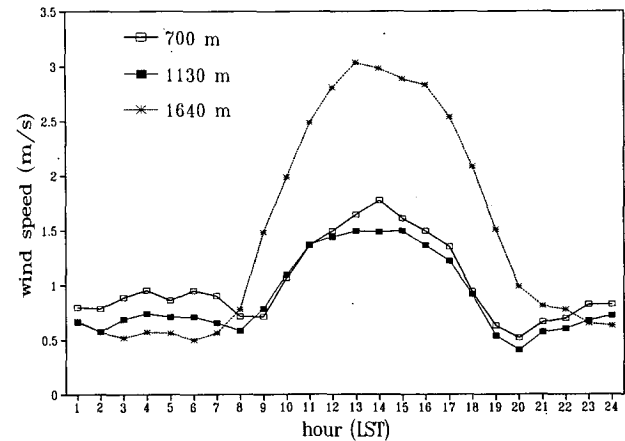


FIG. 6. Average diurnal wind speed for July 1992. Typical of all months with stronger upslope daytime winds and lighter nighttime drainage wind.

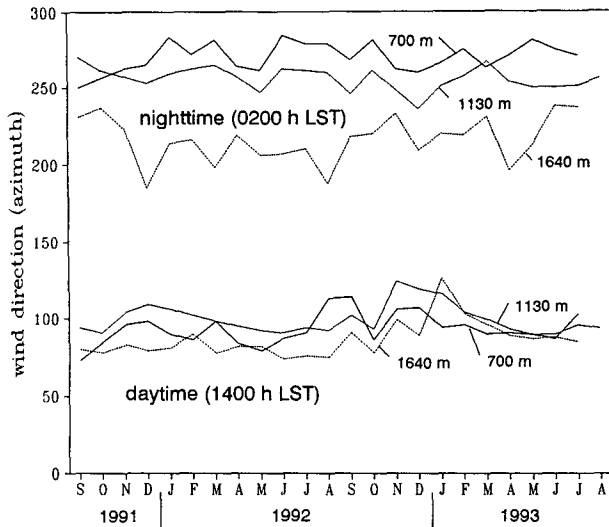


FIG. 7. Average monthly wind direction at 0200 and 1400 LST, showing the consistent diurnal wind direction reversal, in conjunction with a thermal wind circulation prevails in all months of the year at all sites on a windward slope facing prevailing easterly winds.

pattern for the transect stations, shown in Fig. 8a for May 1993, includes a midmorning minimum and late afternoon maximum at the lower sites and a more even distribution at the upper station. A secondary nocturnal maximum is also well developed at the lowest site (700 m) and is consistent with the adjacent open ocean diurnal rainfall pattern.

Leaf wetness showed a strong diurnal pattern as shown in Fig. 8b, with daytime minima and nighttime maxima. This cycle more closely matched the diurnal relative humidity curve than the rainfall pattern, suggesting the importance of nighttime condensation (dew) as a major contributor to leaf wetness for windward forest sites.

Relative humidity followed a typical sea level pattern with daytime minima and nighttime maxima (Fig. 8c), in opposition to air temperature. Average humidity values were high for all sites, including the 1640-m station, near the inversion level. Although several months of humidity data for 1992 are suspect, even the lowest values are near the average relative humidity of 79.0% reported for leeward Haleakalā, Maui, at the same elevation (Giambelluca and Nullet 1991).

Estimated evaporation for the transect was about 10% higher than measured evaporation reported over a comparable transect on windward Mauna Loa by Bean et al. (1994), as shown in Fig. 9, although the altitudinal profile pattern is identical. Below-normal rainfall for the period of measurement, and correspondingly higher solar radiation (as suggested above with respect to 1979 measurements), could account for the higher Penman-Monteith evaporation estimates.

5. Conclusions

The study has confirmed, with the first long-term climate measurements over a wet, windward slope on Hawaii, what previous short-term measurement have suggested, and has added new, quantitative information on variables such as soil temperature, leaf wetness, PAR, and solar radiation. The transect measurements clearly indicate a dominant characteristic climate on Mauna Loa's wet windward slope that extends nearly

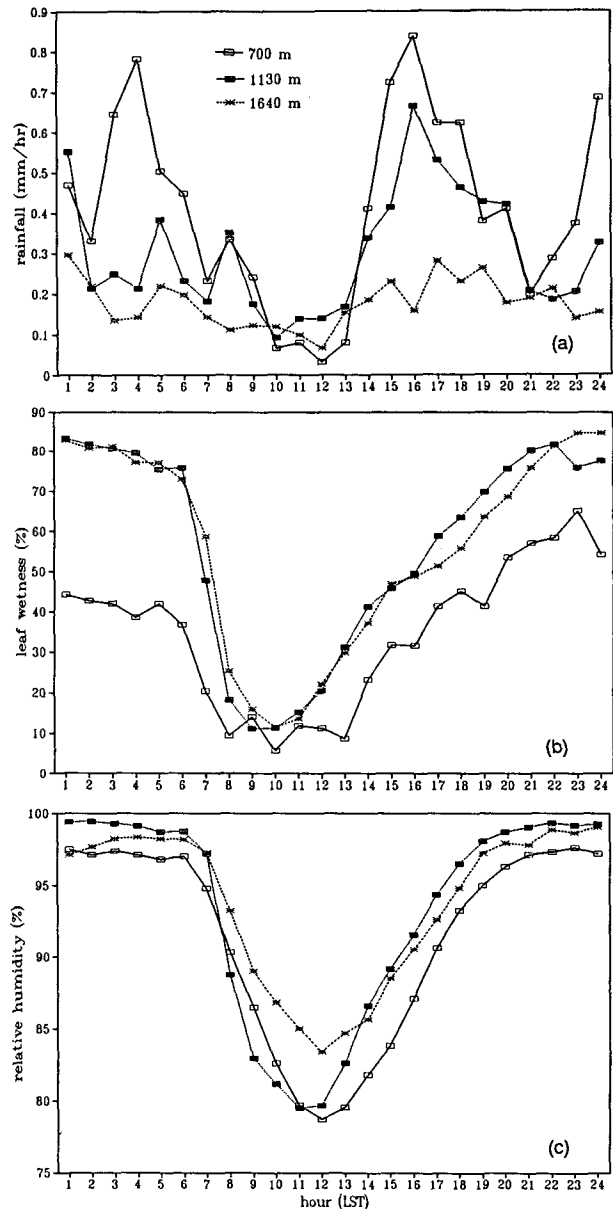


FIG. 8. (a) Diurnal rainfall, (b) leaf wetness, and (c) relative humidity patterns for May 1993. Sites at 700 and 1130 m typically have afternoon rainfall maxima and midmorning minima (secondary nighttime maxima at 700 m), while rainfall is more evenly distributed throughout the day at 1640 m. Leaf wetness more closely corresponds to the relative humidity curve than to the rainfall distribution.

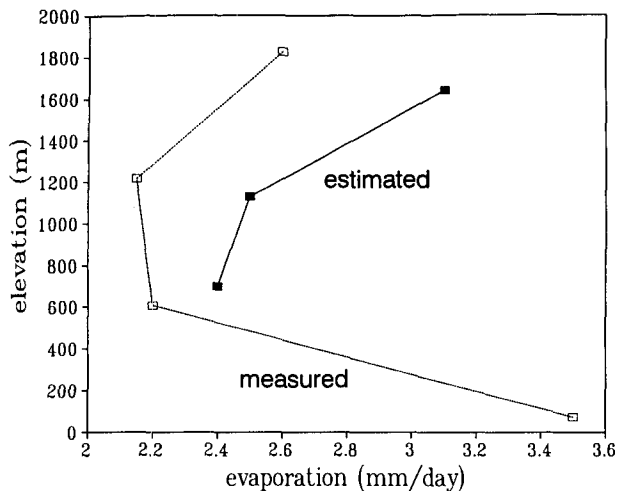


FIG. 9. Estimated evaporation for the period of measurement compared to measured evaporation for various intervals during 1984–87 on windward Mauna Loa (Bean et al. 1994). Slightly higher estimated evaporation values may be related to below-normal rainfall for the measurement period.

to the trade-wind inversion level. Although the absolute values differ, diurnal and annual patterns of all climate elements measured along the approximately 1-km elevation transect are virtually identical, with only minor differences. The surface wind reverses in direction each day at all elevations, with a slightly greater southerly component in the nighttime drainage wind at higher elevations. The temperature range and lapse rate remain constant with elevation, with the exception of soil temperatures at 1640 m. Relative humidity varies little over the range of the transect, and diurnal leaf wetness follows the relative humidity pattern at all sites. PAR remains a constant fraction of solar radiation at each site, with the fraction declining about 4% between 700 and 1640 m. No clear differences in the annual or diurnal solar radiation cycles are apparent, with winter values being about two-thirds of summer values and a diurnal cycle symmetric around local noon.

Limitations on available soil moisture due to the lack of significant storage on the young volcanic surface of the 1855 lava flow were most pronounced at the highest site (1640 m) where total two-year rainfall of 2896 mm (about one-half normal) was near estimated evaporation for the period of 2263 mm. At lower sites, higher rainfall and lower estimated evaporation suggest large moisture surpluses even during below-normal rainfall periods. (For example, at the 700-m station, rainfall for the period was nearly four times evaporation.) These water balance differences along the elevation gradient help explain the variation in biomass accumulation between sites (see Fig. 2) since 1855.

Acknowledgments. We would like to thank Richard Mitsutani of the National Weather Service for providing the Hilo climate data. Financial support was provided by the National Science Foundation through Grant DEB 89-18526 (Ecosystem Dynamics in Hawaii), principal investigator D. Mueller-Dombois. Thank you Kathy Hughes and Gordon Segal for providing data collection and data processing support.

REFERENCES

- Armstrong, R. W., 1983: *Atlas of Hawaii*. 2d ed. University of Hawaii Press, 238 pp.
- Bean, C., J. O. Juvik, and D. Nullet, 1994: Mountain evaporation profiles on the Island of Hawai'i. *J. Hydrol.*, **156**, 181–192.
- Blumenstock, D. I., and S. Price, 1967: *Climates of the states: Hawaii*. Climatography of the United States, No. 60-51, U.S. Dept. of Commerce, 27 pp.
- Chu, P.-S., 1989: Hawaiian drought and the Southern Oscillation. *Int. J. Climatol.*, **9**, 619–631.
- Eber, L. E., 1957: Upper air and surface wind observations in Project Shower. *Tellus*, **9**, 558–568.
- Ekern, P. C., 1965: The fraction of sunlight retained as net radiation in Hawaii. *J. Geophys. Res.*, **70**(4), 785–793.
- Garrett, A. J., 1980: Orographic cloud over the eastern slopes of Mauna Loa volcano, Hawaii, related to insolation and wind. *Mon. Weather Rev.*, **108**, 931–941.
- Giambelluca, T. W., and D. Nullet, 1991: Influence of the trade wind inversion on the climate of a leeward mountain slope in Hawaii. *Climate Res.*, **1**, 207–216.
- , M. A. Nullet, and T. A. Schroeder, 1986: Rainfall atlas of Hawaii. Dept. of Land and Natural Resources Report R76, State of Hawaii, Honolulu, Hawaii, 267 pp.
- How, K. T. S., 1978: Solar radiation in Hawaii, 1932–1975. Dept. of Land and Natural Resources Report R57, State of Hawaii, Honolulu, Hawaii, 99 pp.
- Jenny, H., 1980: *Soil Genesis with Ecological Perspectives*. Springer-Verlag, 560 pp.
- Juvik, J. O., D. C. Singleton, and G. G. Clarke, 1978: Climate and water balance on the island of Hawaii. Mauna Loa 20th Anniversary Report, NOAA, 158 pp.
- , D. Nullet, P. Banko, and K. Hughes, 1993: Forest climatology near the tree line in Hawaii. *Agric. For. Meteorol.*, **66**, 159–172.
- Lavoie, R. L., 1967a: Background data for the warm rain project. *Tellus*, **19**, 348–353.
- , 1967b: Air motions over the windward coast of the Island of Hawaii. *Tellus*, **19**, 354–358.
- Leopold, L. B., 1949: The interaction of trade wind and sea breeze, Hawaii. *J. Meteorol.*, **6**, 312–320.
- Mendonça, B. G., 1969: Local wind circulation on the slopes of Mauna Loa. *J. Appl. Meteorol.*, **8**, 533–541.
- Monteith, J. L., 1965: Evaporation and environment. *The State and Movement of Water in Living Organisms, Symp. Society for Experimental Biology*, Swansea, Great Britain, 205–234.
- Mordy, W. A., 1957: Geographic and climatic notes on the Project Shower area. *Tellus*, **9**, 472–474.
- Mueller-Dombois, D., 1992: Distributional dynamics of Hawaiian vegetation. *Pacific Science*, **46**(2), 221–231.
- Nullet, D., and T. W. Giambelluca, 1990: Winter evaporation on a mountain slope, Hawaii. *J. Hydrol.*, **112**, 257–265.
- Schroeder, T., 1974: Climate controls. *Prevailing Trade Winds*, M. Sanderson, Ed., University of Hawaii Press, 12–36.
- Vitousek, P. M., G. Aplet, D. R. Turner, and J. J. Lockwood, 1992: The Mauna Loa environmental matrix: Foliar and soil nutrients. *Oecologia*, **89**, 272–282.